CardioRenal Medicine

Cardiorenal Med 2020;10:42–50
DOI: 10.1159/000503224
Received: July 2, 2019
Accepted: September 5, 2019
Published online: November 6, 2019

Research Article

Mitochondrial-Derived Peptide MOTS-c Attenuates Vascular Calcification and Secondary Myocardial Remodeling via Adenosine Monophosphate-Activated Protein Kinase Signaling Pathway

Ming Wei[a, e, f] Lu Gan[b] Zheng Liu[c] Li Liu[d] Jin-Rui Chang[a]
Da-Chuan Yin[e] Hui-Ling Cao[e] Xing-Li Su[a, f] Wanli W. Smith[g]

[a]Department of Pharmacology, Xi'an Medical University, Xi'an, China; [b]Department of Gynecology, Shaanxi Provincial People's Hospital, The Third Affiliated Hospital of Xi'an Jiaotong University, Xi'an, China; [c]College of Medical Laboratory Science, Guilin Medical University, Guilin, China; [d]Ultrasound Diagnostics Department, Shaanxi Provincial People's Hospital, Xi'an, China; [e]Shaanxi Key Laboratory of Ischemic Cardiovascular Disease, Xi'an Medical University, Xi'an, China; [f]Shaanxi Key Laboratory of Brain Disorders, Xi'an Medical University, Xi'an, China; [g]Department of Psychiatry and Behavioral Sciences, Johns Hopkins University School of Medicine, Baltimore, MD, USA

Keywords
Adenosine monophosphate-activated protein kinase · Angiotensin II type 1 · Endothelin B · MOTS-c · Rat model of vascular calcification

Abstract
Introduction: Vascular calcification (VC) is a complex, regulated process involved in many disease entities. So far, there are no treatments to reverse it. Exploring novel strategies to prevent VC is important and necessary for VC-related disease intervention. ***Objective:*** In this study, we evaluated whether MOTS-c, a novel mitochondria-related 16-aa peptide, can reduce vitamin D3 and nicotine-induced VC in rats. ***Methods:*** Vitamin D3 plus nicotine-treated rats were injected with MOTS-c at a dose of 5 mg/kg once a day for 4 weeks. Blood pressure, heart rate, and body weight were measured, and echocardiography was performed. The expression of phosphorylated adenosine monophosphate-activated protein kinase (AMPK) and the angiotensin II type 1 (AT-1) and endothelin B (ET-B) receptors was determined by Western blot analysis. ***Results:*** Our results showed that MOTS-c treatment significantly attenuated VC. Fur-

M.W., L.G., and Z.L. contributed equally to this work.

Prof. Xing-Li Su
Department of Pharmacology
Xi'an Medical University, No. 1 Xinwang Road
Weiyang District, Xi'an, Shaanxi 710021 (China)
E-Mail suxingli@xiyi.edu.cn

Da-Chuan Yin or Hui-Ling Cao
Shaanxi Key Laboratory of Ischemic Cardiovascular Disease
Xi'an Medical University
Xi'an 710021 (China)
E-Mail yindc@nwpu.edu.cn or caohuiling_jzs@xiyi.edu.cn

thermore, we found that the level of phosphorylated AMPK was increased and the expression levels of the AT-1 and ET-B receptors were decreased after MOTS-c treatment. ***Conclusions:*** Our findings provide evidence that MOTS-c may act as an inhibitor of VC by activating the AMPK signaling pathway and suppressing the expression of the AT-1 and ET-B receptors.

Introduction

Vascular calcification (VC) is the pathological accumulation of calcium phosphate crystal deposits in the medial and intimal layers of the vessel wall, and it complicates the progression of many diseases and worsens the prognosis of chronic kidney disease, cardiac valve disease, and atherosclerosis [1]. Patients with VC exhibit an increased risk of cardiovascular events, and so far, no treatments have been found to reverse it [2]. VC often occurs in 2 areas of the vessel wall, the intima, and the media [3]. The intimal layer of the artery is comprised of endothelial cells surrounded by a thick outer layer of elastic fibers [4]. Calcification at this site is associated with dyslipidemia and inflammation that results in the thickening of the intimal layer and leads to atherosclerosis [5]. Medial calcification mainly occurs in an environment without inflammatory cell infiltration or lipid deposition [5].

Increasing evidence has demonstrated that adenosine monophosphate-activated protein kinase (AMPK) signaling plays critical roles in regulating VC formation and vascular homeostasis [6–9]. Furthermore, angiotensin II type 1 (AT-1) and endothelin B (ET-B) have been found to be involved in the AMPK pathway by binding to the AT-1 and ET-B receptors, respectively [10, 11]. Recently, MOTS-c, a novel bioactive mitochondrial-derived peptide, has been demonstrated to activate the AMPK pathway to promote metabolic homeostasis [12]. Thus, in this study, we set out to evaluate a novel strategy to modulate VC. We used a rat model of vitamin D3 plus nicotine (VDN)-induced VC and various biochemical and pathological approaches to study the actions of MOTS-c. Our study provides a potential novel strategy for blocking VC.

Material and Methods

Synthesis of the MOTS-c Peptide

MOTS-c was composed of Met, Arg, Trp, Gln, Glu, Met, Gly, Tyr, Ile, Phe, Tyr, Pro, Arg, Lys, Leu, and Arg residues, which were synthesized by China Peptides Co., Ltd. with over >98% purity. The peptides were dissolved in ddH_2O, and aliquots were frozen at –20 °C until use.

Animals and the VC Rat Model

Forty male Sprague-Dawley rats (190–210 g) were obtained from the Animal Center of Fourth Military Medical University. All animals received humane care, and the experimental protocols were approved by the Animal Care and Use Committee of Xi'an Medical University. Rats were randomly divided into 4 groups (n = 10 rats per group): the control (saline) group, the control (5 mg/kg MOTS-c) group, the VDN (VDN + saline) group, and the MOTS-c (VDN + 5 mg/kg MOTS-c) group. The rats were intramuscularly injected with vitamin D3 (300,000 IU/kg) and intragastrically administered nicotine (5 mL/kg) in peanut oil for 4 weeks. The mice were also intraperitoneally injected with MOTS-c every day for 4 weeks.

Measurement of Blood Pressure, Heart Rate, Body Weight, and Echocardiographic Parameters

Heart rate, systolic blood pressure (SBP), and diastolic blood pressure (DBP) were measured with a noninvasive tail-cuff system. SBP and DBP were used to calculate the pulse pressure. All data were the average of 5 consecutive cardiac cycles. Wall thickness and left ventricular (LV) dimensions were obtained from a long-axis view at the level of the chordae tendineae. The LV end-diastolic diameter, LV end-diastolic posterior wall thickness, and septum thickness were measured by echocardiography.

Vascular Ring Analysis

At the end of the experiment, animals were sacrificed by CO_2 inhalation. The superior mesenteric artery was removed from adhering tissue under a dissecting microscope. The vessels were then cut into cylindrical segments of 2–3 mm in length. The segments were immersed in PSS (5 mL) at 37 °C. The solution was continuously aerated with gas (containing 5% CO_2 and 95% O_2) until it reached a pH of 7.4. Following the mounting of the arterial segments, isometric tension was continuously recorded by using Chart software (AD Instruments, UK). The segments were stabilized at a resting tone (2 mN) for at least 1.5 hand then immersed in a K^+-rich (60 mM) solution to reach a final K^+ concentration of 60 mM. The high K+ physiological salt solution (KPSS) induced the constriction of the mouse vasculature. Acetylcholine (10 μM) was added after precontraction with KPSS to test the responsiveness of the vasculature to vasoconstrictors. Vascular tension analysis was performed using a 4-channel vascular tension detector (DMT, Denmark).

Alkaline Phosphatase Activity Assay and the Quantification of Calcium Content in the Aorta

Abdominal aortic blood was collected. The plasma was separated after centrifugation at 3,000 rpm for 15 min at 4 °C. Aortic tissues were homogenized in ice-cold buffer (20 mmol/L HEPES, 0.2% NP-40, and 20 mmol/L $MgCl_2$, pH 7.4). After centrifugation at 8,000 rpm for 10 min, the supernatant was collected. Alkaline phosphatase (ALP) activity was measured by using the ALP assay kit. ALP activity in the aorta was normalized to total protein levels, as determined by the Bradford method. The aortic segments were dried at 55 °C, weighed, dissolved in HNO_3, dried at 180 °C, and redissolved in a blank solution (27 nmol/L KCl and 27 μmol/L $LaCl_3$). Calcium levels were determined by a colorimetry assay through a reaction with o-cresolphthalein complexone and normalized to the aortic dry weight.

Hematoxylin-Eosin, Alizarin Red S, and von Kossa Staining

Thoracic aortic tissues were fixed using 10% formalin, dehydrated, and embedded in paraffin. Some sections were stained with hematoxylin-eosin. Some sections were stained with 1% Alizarin Red S (Sigma, Shanghai, China) for 30 min and washed with 0.2% acetic acid. Some sections were dehydrated before incubation in 1.5% silver nitrate solution for 1 h in sunlight and then immersed in 5% sodium thiosulfate for 2 min followed by counterstaining with safranine (red staining). Images were taken under a light microscope and analyzed by investigators blinded to the treatment conditions.

Western Blot Analysis

Proteins were separated by 10–12% SDS-polyacrylamide gel electrophoresis and transferred to a polyvinylidene difluoride membrane. Anti-phospho-AMPK (Thr172), anti-AMPK, anti-AT-1 receptor, anti-ET-B receptor, and anti-β-actin (Beijing Zhong Shan Golden Bridge Biological Technology, China) antibodies were used as primary antibodies, and horseradish peroxidase-conjugated anti-mouse and anti-rabbit antibodies were used as secondary antibodies (Abcam, Cambridge, UK). Immunoreactive bands were visualized using the ECL kit (Amersham Pharmacia, New Jersey), and images were obtained using the ChemiDoc™ Touch Imaging System (Bio-Rad, Hercules, CA, USA).

Statistical Analysis

The data are reported as the mean ± SD. Differences between multiple groups were analyzed by one-way ANOVA followed by post hoc individual comparisons. Differences were considered statistically significant at $p < 0.05$. All statistical analyses were performed by using SPSS20.0 (SPSS Inc., Chicago, IL, USA).

Results

MOTS-c Improved Vitamin D3- and Nicotine-Induced Abnormal Blood Pressure and Echocardiographic Parameters

The body weight (BW), blood pressure, heart rate, and cardiac structure of the rats were measured before and after 4 weeks of MOTS-c treatment. Before MOTS-c treatment, blood pressure, BW, and cardiac structure were not different among these 4 groups. Echocardiography showed that the LV internal diameter at diastole (LVIDd) and systole (LVIDs) in the VDN group were lower compared to those in the control group. The LV posterior wall thickness

Table 1. MOTS-c reversed VDN-induced abnormal chocardiographic parameter changes

Characteristics	CON	CON + MOTS-c	VDN	VDN + MOTS-c
IVSd, mm	2.07±0.57	2.11±0.45	2.95±0.23[a, *]	2.09±0.12[b, *]
LVIDd, mm	6.67±0.4	6.73±0.43	4.25±0.65[a, *]	6.65±0.38
LVIDs, mm	2.33±0.73	2.17±0.31	1.31±0.16[a, *]	2.70±9.36
LVPWd, mm	2.39±0.73	2.13±0.11	3.98±0.16[a, *]	2.61±0.86[b, *]
LVPWs, mm	3.83±0.51	4.03±0.32	4.58±0.16	4.10±0.36
LVvold, μL	233.21±26.73	222.13±21.31	85.38±4.16[a, *]	227.0±6.36[b, *]
LVvols, μL	28.33±2.73	27.13±2.31	4.38±1.16[a, *]	25.70±1.36[b, *]
LVmass, mg	870.33±55.73	859.13±0.31	1,061.38±0.16[a, *]	962.70±9.36[b, *]
LVmass/BW, mg/g	2.33±0.73	2.13±0.31	3.38±0.16[a, *]	3.70±0.36[b, *]

Data are mean ± SD, n =10 per group. IVSd, end-diastolic septal thickness; LVIDd, left ventricular internal diastolic diameter; LVIDs, left ventricular end systolic diameter; LVPWd, left ventricular posterior wall thickness at end diastole; LVPWs, left ventricular posterior wall thickness at end systole; LVvold, left ventricular volume at end diastole; LVvols, left ventricular volume at end systole; LVmass, left ventricular mass; BW, body weight; VDN, vitamin D3 plus nicotine; CON, control. [a] VDN versus CON. [b] VDN versus VDN+MOTS-c. * $p < 0.05$.

Table 2. MOTS-c reversed VDN-induced SBP and DBP elevation

Characteristics	CON	CON + MOTS-c	VDN	VDN + MOTS-c
BW, g	349.67±14.57	336.67±12.50	312.28±12.23[a, *]	315.56±12.20[b, *]
SBP, mm Hg	103.67±4.73	105.47±4.63	126.25±5.65[a, *]	108.20±6.38[b, *]
DBP, mm Hg	71.33±4.73	72.37±5.13	95.38±3.16[a, *]	78.20±9.36[b, *]

Data are mean ± SD, n = 10 per group. BW, body weight; SBP, systolic blood pressure; DBP, diastolic blood pressure; VDN, vitamin D3 plus nicotine; CON, control. [a] VDN versus CON. [b] VDN versus VDN+MOTS-c. * $p < 0.05$.

and LV mass/BW ratio were higher than those in the control group, indicating that there was clear hypertrophy in the left ventricle in this VC model. After MOTS-c treatment, the LVIDd and LVIDs were increased, and the LV posterior wall thickness and LV mass/body weight ratio were reversed compared with those in the untreated rats (Table 1). MOTS-c treatment also significantly reduced VDN-induced SBP and DBP elevation (Table 2). There were no significant changes in heart rate, pulse pressure, or BW among the 4 experimental groups.

MOTS-c Increased Vascular Tension

As shown in Figure 1a, the vascular tension in the VDN group was significantly reduced compared with that in the control group and the VDN + MOTS-c intervention group ($p < 0.01$). Furthermore, as shown in Figure 1b, treatment with KPSS, KPSS+ACh, or MOTS-c significantly relaxed the ACh- and KPSS-induced constriction of the superior mesenteric artery in the mice. Figure 1c shows the results of vascular tension after treatment with KPSS or KPSS+ACh. In our VDN group, there was a significant decrease invascular attenuation (approximately 0.7 mN) compared with that in the sham control group (approximately 3.8 mN) and the VDN +MOTS-c group (approximately 3.4 mN).

MOTS-c Inhibited VC

To further assess VC pathology, we measured the calcium content (Fig. 2a) and ALP activity (Fig. 2b) in the aorta. The VDN group showed a 2- to 3-fold increase in calcium content

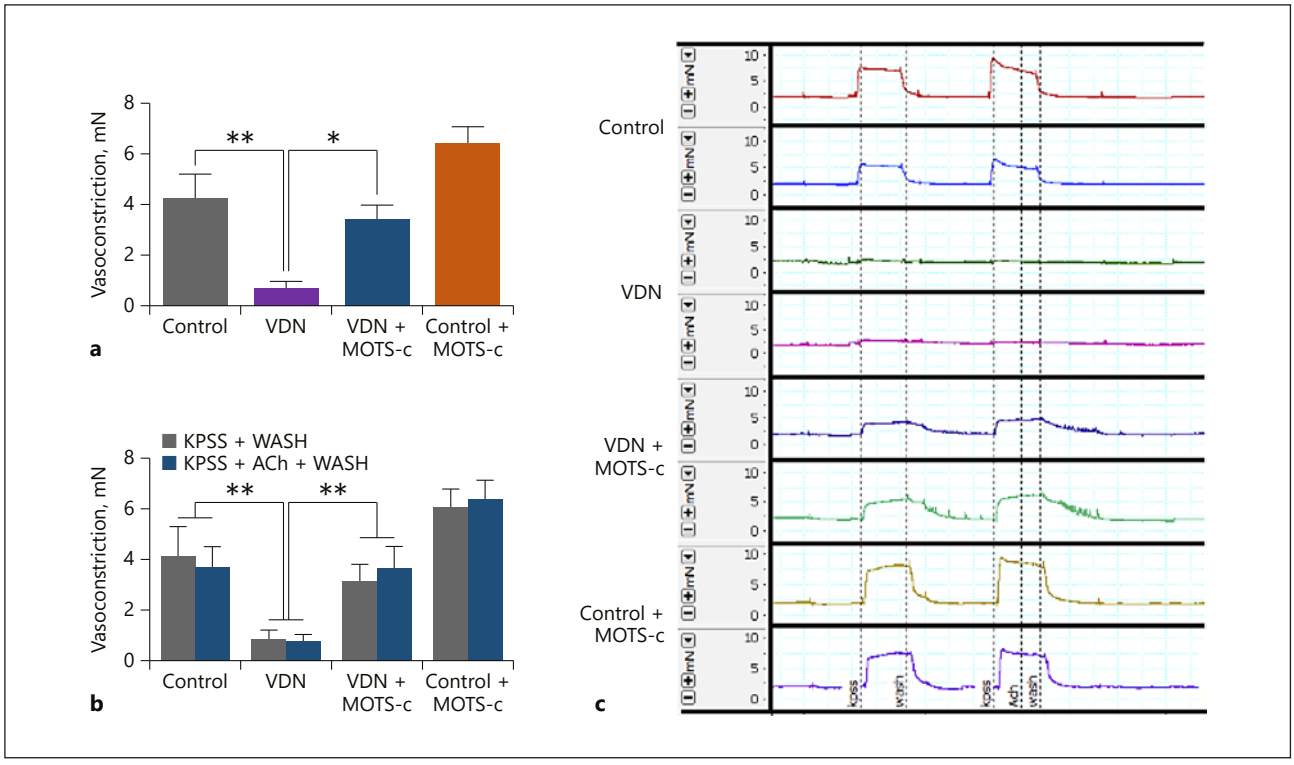

Fig. 1. MOTS-c (5 mg/kg) reduced vascular tension and improved echocardiographic parameters under VC conditions. **a** Quantitative analysis of vascular tension in the control, control + MOTS-c, VDN, and VDN + MOTS-c groups. VDN vs. MOTS-c and VDN vs. VDN + MOTS-c. **b** Quantitative analysis of vascular tension after the addition of KPSS and Ach to the control, control + MOTS-c, VDN, and VDN + MOTS-c groups. **c** Vascular tension was monitored by echocardiography after the addition of KPSS to the control, control + MOTS-c, VDN, and VDN + MOTS-c groups. Statistical significance is shown as * $p < 0.05$ and ** $p < 0.01$, and the data were analyzed by ANOVA. VDN, vitamin D3 plus nicotine; KPSS, K^+ physiological salt solution; ACh, acetylcholine.

and ALP activity in the aorta compared with those in the sham control group. Treatment with MOTS-c significantly reduced the VDN-induced elevation in calcium content and ALP activity by 55.7% ($p < 0.01$) and 50.1% ($p < 0.01$), respectively. Furthermore, hematoxylin-eosin staining revealed robustly disordered elastic fibers in the calcified aortas of the VDN group rats. In contrast, MOTS-c treatment dramatically reduced the number of disordered elastic fibers and significantly improved vascular wall structure (Fig. 2c). Moreover, MOTS-c also significantly reduced VDN-induced calcium phosphate salt deposition in the calcified aortas, as detected by alizarin red S staining and von Kossa staining.

MOTS-s Increased the VDN-Induced Reduction in AMPK Phosphorylation

AMPK signaling plays a critical role in vascular system function [6]. We found that AMPK phosphorylation levels were significantly reduced in the aortas of VDN rats compared with sham control rats (Fig. 3a). After 4 weeks of MOTS-c treatment, the phosphorylation level of AMPK was reversed. In Figure 3b and a histogram is used to represent changes in the Western blot results. The level of phosphorylated-AMPK (p-AMPK) in the VDN group was lower than that in the control group, indicating that the expression of p-AMPK was decreased upon VDN treatment. In the VDN group, the level of p-AMPK was increased after the addition of MOTS-c, suggesting that MOTS-c can reverse the expression of p-AMPK.

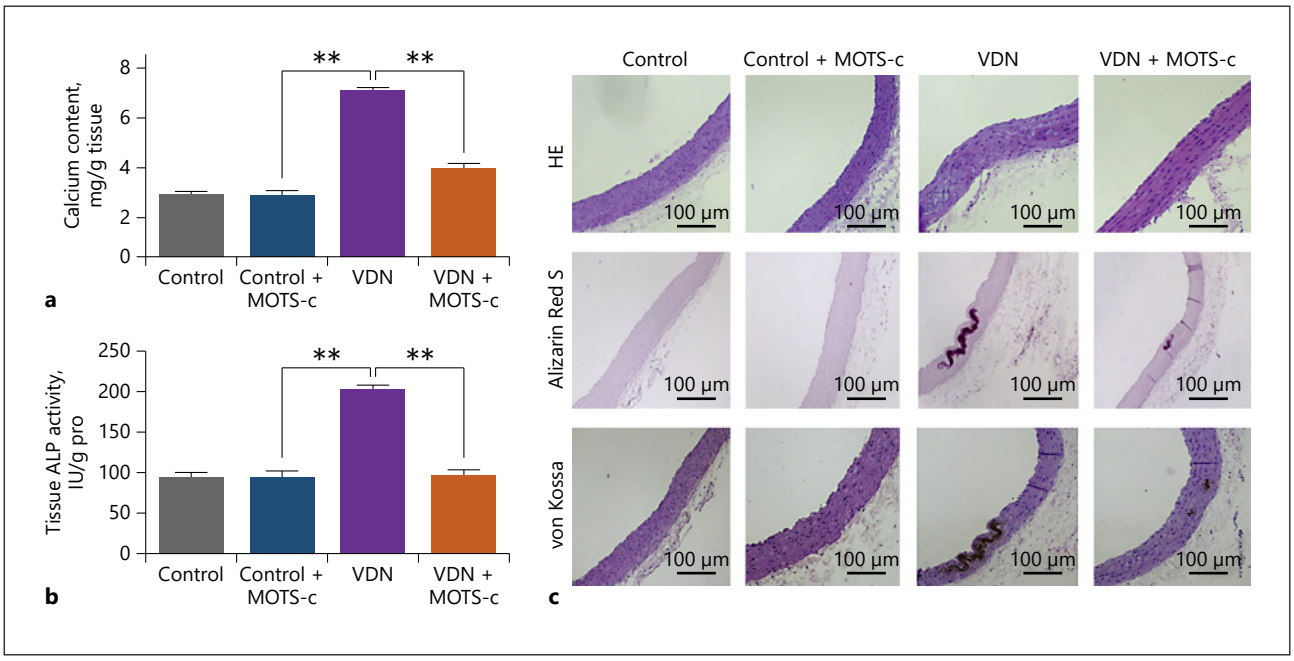

Color version available online

Fig. 2. MOTS-s improved VDN-induced VC in the rat aorta. **a**, **b** Calcium content (**a**) and ALP activity (**b**) in VDN rat aortas. The data are presented as the mean ± SD (n = 10). **c** Hematoxylin-eosin staining, Alizarin Red S, and von Kossa staining of VDN rat aortas. Scale bars, 100 μm. Original magnification, ×100. Statistical significance is shown as ** $p < 0.01$, and the data were analyzed by ANOVA. ALP, alkaline phosphatase; HE, hematoxylin-eosin; VDN, vitamin D3 plus nicotine.

The Expression Levels of the ET-B and AT-1 Receptors Were Decreased after MOTS-c Treatment

We also found that the expression levels of the ET-B and AT-1 receptors in the VDN group were increased compared to those in the control group and were decreased after MOTS-c treatment (Fig. 4). Taken together, these results demonstrate that the AMPK/AT-1/ET-B signaling pathway regulates VC formation.

Discussion

MOTS-c is a 16-aa peptide encoded within the 12S rRNA locus of mtDNA. It can improve insulin sensitivity and maintain metabolic homeostasis within and between cells [12]. In mice, MOTS-c treatment alleviates high fat diet-induced obesity and insulin resistance [13]. In humans, lower levels of circulating endogenous MOTS-c are associated with impaired coronary endothelial function [14]. In our study, we established a VC rat model with decreased vascular tension, increased blood pressure, and calcium deposition in the aorta by feeding rats vitamin D3 and nicotine. Treatment with MOTS-c significantly decreased blood pressure, maintained normal cardiac structure, reversed ventricular remodeling, and reduced the stiffness of blood vessels in VDN-treated rats. SBP and DBP were also decreased in MOTS-c-treated VDN-treated rats. Moreover, there was also an improvement in the restoration of heart function in terms of the LVIDd and LVIDs after MOTS-c treatment. Consistent with previous reports, we demonstrated that MOTS-c can improve the condition of VDN-induced vascular and heart abnormalities.

Previous reports have shown that MOTS-c can amplify glucose uptake, inhibit the folate cycle and de novo purine biosynthesis following metabolic stress, and regulate nuclear gene

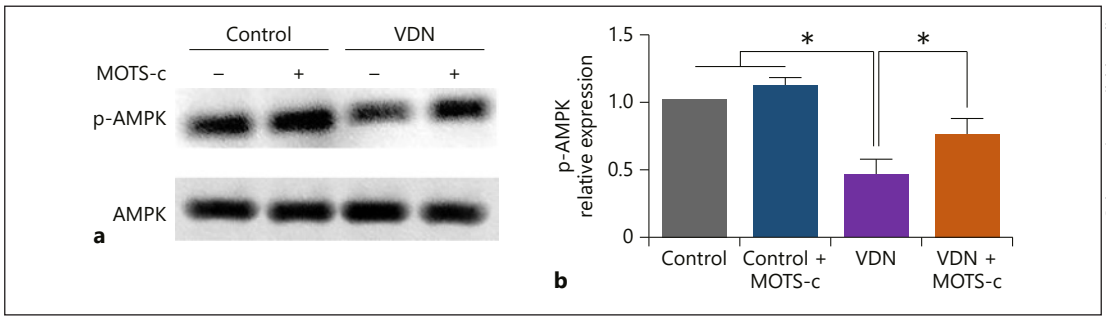

Fig. 3. MOTS-s increased the expression of p-AMPK. **a** The expression of p-AMPK was analyzed by Western blotting of the 4 experimental groups: the control group, the control + MOTS-c group, the VDN group, and the VDN + MOTS-c group. **b** Quantification of the Western blotting results. The data are presented as the mean ± SD (n = 3). Statistical significance is shown as * $p < 0.05$, and the data were analyzed by ANOVA. VDN, vitamin D3 plus nicotine; AMPK, adenosine monophosphate-activated protein kinase; p-AMPK, phosphorylated-AMPK.

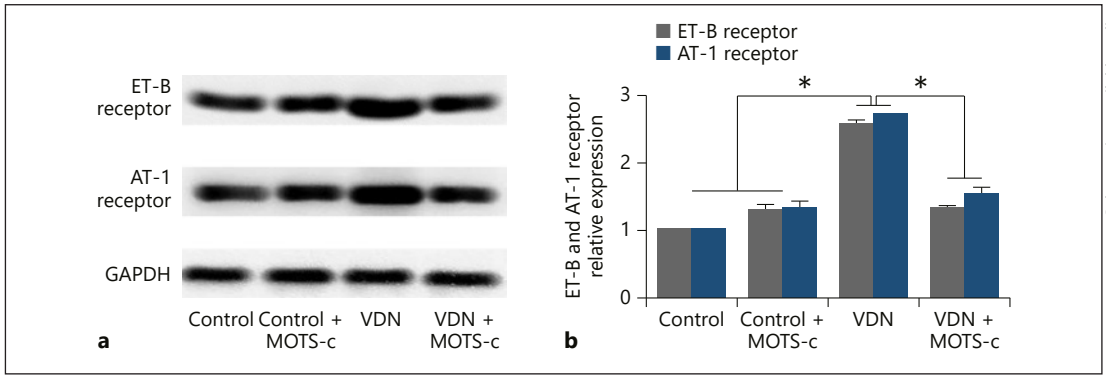

Fig. 4. MOTS-c reversed VDN-induced elevations in the ET-B and AT-1 receptors. **a** The expression levels of the ET-B and AT-1 receptors were measured by Western blot analysis. **b** Quantification of the Western blotting results. The data are presented as the mean ± SD (n = 3). Statistical significance is shown as * $p < 0.05$, and the data were analyzed by ANOVA. VDN, vitamin D3 plus nicotine; ET-B, endothelin-b; AT-1, angiotensin type-1.

expression in an AMPK-dependent manner [15]. Our results showed that MOTS-c reverses VDN-induced AMPK downregulation. In 2016, Zhang et al. [7] demonstrated that metformin alleviates VC and suppresses calcium deposition in the tunica media in VDN-treated rats via the AMPK pathway [16]. Li et al. [9] found that through activating AMPK signaling, death-associated protein kinase 3 modulates vascular smooth muscle cell calcification. In mice with hypoxia-induced pulmonary hypertension, the activation of the AMPK pathway can effectively improve right ventricular systolic pressure and right ventricular hypertrophy due to treatment with liraglutide. Here, we demonstrated that treatment with MOTS-c reversed VDN-induced VC pathology by increasing AMPK signaling activation. We hypothesize that MOTS-c has a similar function as metformin in alleviating VC, but further experiments are required for confirmation.

Our results also demonstrated that MOTS-c decreased the levels of the AT-1 and ET-B receptors. AT-1 and ET-B have been found to be involved in the AMPK pathway by binding to the AT-1 and ET-B receptors, respectively. A decreased level of the AT-1 receptor plays roles in reducing oxidative stress and preventing the development of myocardial contractile dysfunction, while a high level of the AT-1 receptor induces myocardial fibrosis and cardiac dysfunction [17, 18]. AT-1 can induce the relocation and suppression of the AMPK pathway via the AT-1 receptor in the development of diabetic proteinuria [19]. After treatment with

metformin, AMPK signaling is activated and AT-1 levels are decreased in the kidney [20]. The endothelins (ETs) are a family of 3 polypeptides (ET-1, ET-2, ET-3), which share structural homology and initiate signaling by binding to G-protein-coupled receptors [21–23]. In epithelial ovarian carcinoma, ET-1 plays a role in epithelial-mesenchymal transition [24]. A decrease in ET-1 receptor activation is beneficial in attenuating biventricular remodeling, and the overexpression of ET-1 causes sustained blood pressure elevation and vascular and renal injury [25]. The activation of the AMPK pathway can also upregulate the ET-B receptor to inhibit autophagy in vascular smooth muscle cells under high glucose conditions [26].

However, there are still some limitations in our study. First, the nicotine/vitamin D model of VC may not be consistency with the common form of progressive atherosclerotic calcification that occurs in humans with diabetes and chronic kidney disease. Second, the myocardial changes may have occurred in part due to reductions in blood pressure.

Conclusions

Taken together, our results demonstrated that MOTS-c improves VDN-induced heart abnormalities and attenuates VC by activating the AMPK pathway and reducing the expression of the AT-1 and ET-B receptors. These findings indicate that MOTS-c maybe a potential anti-calcification agent for VC intervention, suggesting that MOTS-c has a beneficial effect against cardiovascular system malfunction.

Acknowledgments

We thank the team at the Animal Center of the Fourth Military Medical University for their support of feeding and injecting the rats.

Statement of Ethics

All animals received humane care, and the experimental protocols were approved by the Animal Care and Use Committee of Xi'an Medical University.

Disclosure Statement

The authors have no conflicts of interest to declare.

Sources of Funding

This study was funded by National Natural Science Foundation of China (81801414, 31400984); the Natural Science Foundation of Guangxi Province (2018JJA140045); the Shaanxi Key Laboratory of Ischemic Cardiovascular Diseases Open Fund (2017ZDKF07); the Open Fund of Shaanxi Key Laboratory for Brain Disorders (18NBZD04); the Supporting Fund Project of Xi'an Medical University in 2017 (2017PT36, 2017PT39,2017PT47); the National Foundation Training Project of Xi'an Medical College in 2017 (2017GJFY34); and the Talent Fund of Xi'an Medical University (2015 RCYJ01).

Author Contributions

M.W., L.G., D.-C.Y., H.-L.C., and X.-L.S.: designed the study. M.W., L.G., Z.L., and L.L.: performed the experiments. M.W., J.-R.C., and W.W.S.: analyzed the data. M.W., L.G., Z.L., X.L.-S., and W.W.S.: wrote the paper with input from all authors.

References

1 Marulanda J, Alqarni S, Murshed M. Mechanisms of vascular calcification and associated diseases. Curr Pharm Des. 2014;20(37):5801–10.
2 Bardeesi AS, Gao J, Zhang K, Yu S, Wei M, Liu P, et al. A novel role of cellular interactions in vascular calcification. J Transl Med. 2017 May;15(1):95.
3 McCullough PA, Chinnaiyan KM, Agrawal V, Danielewicz E, Abela GS. Amplification of atherosclerotic calcification and Mönckeberg's sclerosis: a spectrum of the same disease process. Adv Chronic Kidney Dis. 2008 Oct;15(4):396–412.
4 Rasheed A, Cummins CL. Beyond the Foam Cell: The Role of LXRs in Preventing Atherogenesis. Int J Mol Sci. 2018 Aug;19(8):2307.
5 Andrews J, Psaltis PJ, Bartolo BA, Nicholls SJ, Puri R. Coronary arterial calcification: A review of mechanisms, promoters and imaging. Trends Cardiovasc Med. 2018 Nov;28(8):491–501.
6 Xu M, Liu L, Song C, Chen W, Gui S. Ghrelin improves vascular autophagy in rats with vascular calcification. Life Sci. 2017 Jun;179:23–9.
7 Zhang X, Xiao J, Li R, Qin X, Wang F, Mao Y, et al. Metformin alleviates vascular calcification induced by vitamin D3 plus nicotine in rats via the AMPK pathway. Vascul Pharmacol. 2016 Jun;81:83–90.
8 Cao X, Li H, Tao H, Wu N, Yu L, Zhang D, et al. Metformin inhibits vascular calcification in female rat aortic smooth muscle cells via the AMPK-eNOS-NO pathway. Endocrinology. 2013 Oct;154(10):3680–9.
9 Li KX, Du Q, Wang HP, Sun HJ. Death-associated protein kinase 3 deficiency alleviates vascular calcification via AMPK-mediated inhibition of endoplasmic reticulum stress. Eur J Pharmacol. 2019 Jun;852:90–8.
10 Kim N, Jung Y, Nam M, Sun Kang M, Lee MK, Cho Y, et al. Angiotensin II affects inflammation mechanisms via AMPK-related signalling pathways in HL-1 atrial myocytes. Sci Rep. 2017 Sep;7(1):10328.
11 Chen Y, Zhang H, Liu H, Li K, Su X. Homocysteine up-regulates ETB receptors via suppression of autophagy in vascular smooth muscle cells. Microvasc Res. 2018 Sep;119:13–21.
12 Lee C, Zeng J, Drew BG, Sallam T, Martin-Montalvo A, Wan J, et al. The mitochondrial-derived peptide MOTS-c promotes metabolic homeostasis and reduces obesity and insulin resistance. Cell Metab. 2015 Mar;21(3):443–54.
13 Yong CQ, Tang BL. A Mitochondrial Encoded Messenger at the Nucleus. Cells. 2018 Aug;7(8):105.
14 Mendelsohn AR, Larrick JW. Mitochondrial-Derived Peptides Exacerbate Senescence. Rejuvenation Res. 2018 Aug;21(4):369–73.
15 Qin Q, Delrio S, Wan J, Jay Widmer R, Cohen P, Lerman LO, et al. Downregulation of circulating MOTS-c levels in patients with coronary endothelial dysfunction. Int J Cardiol. 2018 Mar;254:23–7.
16 Kim KH, Son JM, Benayoun BA, Lee C. The Mitochondrial-Encoded Peptide MOTS-c Translocates to the Nucleus to Regulate Nuclear Gene Expression in Response to Metabolic Stress. Cell Metab. 2018 Sep;28(3):516–524.e7.
17 Honda J, Kimura T, Sakai S, Maruyama H, Tajiri K, Murakoshi N, et al. The glucagon-like peptide-1 receptor agonist liraglutide improves hypoxia-induced pulmonary hypertension in mice partly via normalization of reduced ET(B) receptor expression. Physiol Res. 2018 Jun;67 Suppl 1:S175–84.
18 Boccellino M, Di Domenico M, Donniacuo M, Bitti G, Gritti G, Ambrosio P, et al. AT1-receptor blockade: protective effects of irbesartan in cardiomyocytes under hypoxic stress. PLoS One. 2018 Oct;13(10):e0202297.
19 Ribeiro RF Jr, Pavan BM, Potratz FF, Fiorim J, Simoes MR, Dias FM, et al. Myocardial contractile dysfunction induced by ovariectomy requires AT1 receptor activation in female rats. Cell Physiol Biochem. 2012;30(1):1–12.
20 Choi JY, Ha TS, Park HY, Ahn HY. Angiotensin II suppresses adenosine monophosphate-activated protein kinase of podocytes via angiotensin II type 1 receptor and mitogen-activated protein kinase signaling. Clin Exp Nephrol. 2013 Feb;17(1):16–23.
21 Deji N, Kume S, Araki S, Isshiki K, Araki H, Chin-Kanasaki M, et al. Role of angiotensin II-mediated AMPK inactivation on obesity-related salt-sensitive hypertension. Biochem Biophys Res Commun. 2012 Feb;418(3):559–64.
22 Rapoport RM, Zuccarello M. Endothelin(A)-endothelin(B) receptor cross talk in endothelin-1-induced contraction of smooth muscle. J Cardiovasc Pharmacol. 2012 Nov;60(5):483–94.
23 Olender J, Nowakowska-Zajdel E, Walkiewicz K, Muc-Wierzgoń M. Endothelins and carcinogenesis. Postepy Hig Med Dosw. 2016 Aug;70(0):872–80.
24 Rosanò L, Cianfrocca R, Spinella F, Di Castro V, Nicotra MR, Lucidi A, et al. Acquisition of chemoresistance and EMT phenotype is linked with activation of the endothelin A receptor pathway in ovarian carcinoma cells. Clin Cancer Res. 2011 Apr;17(8):2350–60.
25 Friedberg MK, Cho MY, Li J, Assad RS, Sun M, Rohailla S, et al. Adverse biventricular remodeling in isolated right ventricular hypertension is mediated by increased transforming growth factor-β1 signaling and is abrogated by angiotensin receptor blockade. Am J Respir Cell Mol Biol. 2013 Dec;49(6):1019–28.
26 Chen Y, Zhang H, Liu H, Li K, Jia M, Su X. High Glucose Upregulated Vascular Smooth Muscle Endothelin Subtype B Receptors via Inhibition of Autophagy in Rat Superior Mesenteric Arteries. Ann Vasc Surg. 2018 Oct;52:207–15.